Heliyon 10 (2024) e39353

Contents lists available at ScienceDirect

Heliyon

journal homepage: www.cell.com/heliyon

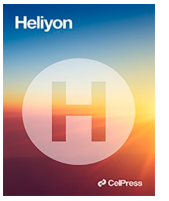

Research article

Effective identification of Alzheimer's disease in mouse models via deep learning and motion analysis

Yuanhao Liang [a,b,c,1], Zhongqing Sun [d,e,1], Kin Chiu [e,f,g,**], Yong Hu [a,b,c,*]

[a] Department of Orthopaedics & Traumatology, School of Clinical Medicine, Li Kai Shing Faculty of Medicine, The University of Hong Kong, Hong Kong SAR, China
[b] Orthopedics Center, The University of Hong Kong-Shenzhen Hospital, Shenzhen, 518053, China
[c] AI and Big Data Lab, The University of Hong Kong-Shenzhen Hospital, Shenzhen, G.D, 518053, China
[d] Department of Neurology, Xijing Hospital, Fourth Military Medical University, Xi'an, 710032, China
[e] Department of Ophthalmology, School of Clinical Medicine, Li Kai Shing Faculty of Medicine, The University of Hong Kong, Hong Kong SAR, China
[f] State Key Lab of Brain and Cognitive Sciences, Li Kai Shing Faculty of Medicine, The University of Hong Kong, Hong Kong SAR, China
[g] Department of Psychology, The University of Hong Kong, Hong Kong SAR, China

A B S T R A C T

Spatial disorientation is an early symptom of Alzheimer's disease (AD). Detecting this impairment effectively in animal models can provide valuable insights into the disease and reduce experimental burdens. We have developed a markerless motion analysis system (MMAS) using deep learning techniques for the Morris water maze test. This system allows for precise analysis of behaviors and body movements from video recordings. Using the MMAS, we identified unilateral head-turning and tail-wagging preferences in AD mice, which distinguished them from wild-type mice with greater accuracy than traditional behavioral parameters. Furthermore, the cumulative turning and wagging angles were linearly correlated with escape latency and cognitive scores, demonstrating comparable effectiveness in differentiating AD mice. These findings underscore the potential of motion analysis as an advanced method for improving the effectiveness, sensitivity, and interpretability of AD mouse identification, ultimately aiding in disease diagnosis and drug development.

1. Introduction

Alzheimer's disease (AD) is a progressive neurodegenerative disorder that can lead to dementia, affecting over 55 million people globally. This widespread impact has heightened the focus on understanding the disease, early diagnosis, and drug development [1–3]. Spatial disorientation and navigation impairments are among the earliest symptoms of AD and can serve as early diagnostic indicators [4,5]. In rodent models, particularly rats and mice, the Morris water maze (MWM) is a widely used behavioral test to evaluate spatial learning and memory in neurodegenerative diseases, especially AD [6,7]. Developed by Richard G. Morris in 1981, the test involves a circular pool filled with opaque water, where animals must swim to find a hidden platform [8]. The rodents learn to use distal and proximal cues to locate the submerged escape platform and navigate directly to it. Spatial learning is assessed through repeated trials,

* Corresponding author. Department of Orthopaedics & Traumatology, School of Clinical Medicine, Li Kai Shing Faculty of Medicine, The University of Hong Kong, SAR Hong Kong, China.
** Corresponding author. Department of Psychology, The University of Hong Kong, Room 409, Hong Kong Jockey Club Building for Interdisciplinary Research, 5 Sassoon Road, Pokfulam, SAR Hong Kong, China.
E-mail addresses: datwai@hku.hk (K. Chiu), yhud@hku.hk (Y. Hu).
[1] These authors contributed equally to this work.

https://doi.org/10.1016/j.heliyon.2024.e39353
Received 24 April 2024; Received in revised form 24 September 2024; Accepted 12 October 2024
Available online 12 October 2024

while reference memory is evaluated based on performance in the platform area when the platform is absent. This test is routinely employed in studies to investigate disease pathogenesis and progression, as well as to evaluate the efficacy of therapeutic interventions [8–10].

With advancements in high-speed video equipment, scientists can now record extensive datasets of animal behavior in exquisite detail during MWM tests. Commercial software such as Smart 3.0, Ethovision (Noldus), AnyMaze (Stoelting Co.), and Top Scan (CleverSys Inc.) are widely used in laboratories to assist with basic mouse tracking and behavior analysis [11]. In recent decades, deep learning-based pose estimation algorithms have significantly advanced markerless human motion analysis. This burgeoning technique allows for the simultaneous tracking of multiple body parts with high accuracy, elevating behavioral analysis to a more detailed level—motion analysis. Several studies have successfully applied human pose estimation to screen neurological disorders such as AD and Parkinson's disease (PD) [12–14]. Concurrently, various well-designed neural networks have been developed for mouse pose estimation [15–17]. These efforts have been applied to mouse behavior and gait analysis in open-field tests for deficit detection, enabling a more detailed understanding and differentiation of movement patterns [18–20]. However, this advanced technique has not been well applied in the MWM swimming conditions, a crucial experiment for understanding behavior and developing drugs for AD [21,22]. To address this gap, we developed a markerless motion analysis system (MMAS). This system enables accurate and automatic detection of the environment and seven distinct body parts, along with a detailed analysis of mouse behaviors and body movements from video recordings. Consequently, it has the potential to enhance the efficiency, sensitivity, and interpretability of behavioral studies in neurological disorders research, compared to current rudimentary tracking methods [11,23].

The performance in MWM is traditionally quantified using parameters such as latency to reach the platform, average speed, average distance from the platform, and swimming distance. While these behavioral parameters provide an overall picture of memory performance, they do not elucidate how an animal solves a spatial task [6,24,25]. Treating the entire body as a single point fails to capture the complexity of searching and swimming behaviors, resulting in a lack of interpretability and robustness. Neurological impairments are expected to directly influence decision-making and movement at every moment, accumulating over time to create behavioral variance. Therefore, motion analysis is anticipated to offer higher sensitivity to spatial disorientations and cognitive deficits. Additionally, functional disturbances such as gait and balance issues are common symptoms observed in AD patients [26–28]. Impaired motor abilities in AD mice have been linked to the development of AD-related pathology, including intraneuronal amyloid-β accumulation, extracellular plaques, increasing myelopathy, and axonal damage in the spinal cord [29–31]. Although immobility and swimming speed are commonly used as control parameters in the MWM test [8], the relationship between motor deficits and cognitive performance in the MWM test requires further exploration. It is crucial to understand how abnormal movements and decisions are made at every moment and how they ultimately lead to behavioral disorders.

2. Results

Our posture and motion analysis method, named MMAS, comprises several modular components. At its core, MMAS utilizes a deep convolutional neural network trained for mouse pose estimation and environment detection in MWM videos. This network identifies 12 two-dimensional markers, or "key points," representing mouse anatomical locations and environmental landmarks, as illustrated in Fig. 1. For each video frame, the mouse's pose and spatial location are detailed. Additionally, we have developed downstream components capable of processing key point time series, determining start and end times, and calculating behavioral and motion parameters. MMAS significantly enhances our ability to perform automatic statistical comparisons on large datasets across various parameters.

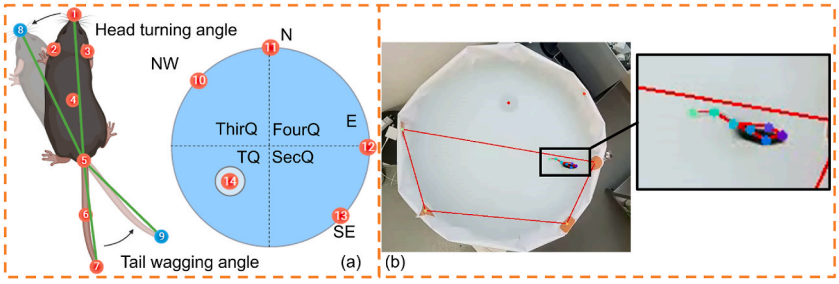

Fig. 1. Diagram of key point detection and the corresponding visualized results. (a) Diagram illustrating the seven critical points of mouse posture and the five essential environmental points in MMAS. The body parts included the nose, left ear, right ear, body center, tail base, mid-tail, and tail tip (points 1–7 in order). The environmental points included the center of the platform (point 14) and four start locations of NW, N, E and SE (points 10–13 in order). The head turning angle (HTA) was defined as the angle created by the nose's position before and after the movement, measured between points 1 and 8, with reference to the butt at point 5. The tail wagging angle (TWA) was similarly defined by the positions of the butt (point 5) and the tail tip before and after the movement (points 7 and 9). The division into four quadrants—TQ, SecQ, ThirQ, and FourQ—on the sixth testing day was defined as illustrated. (b) The tracking results visualized in our experimental videos.

2.1. Pose estimation and environment detection

A total of 27 wild-type (WT) mice (12 males and 15 females) and 20 AD mice (11 males and 9 females) were included in this study. Following five days of training and a sixth day of testing, approximately 1000 experimental videos were recorded at a resolution of 640 × 480 pixels and a frame rate of 30 fps. We automatically extracted 1500 keyframes using k-means clustering for the dataset, which were then manually labeled by an experienced researcher. As illustrated in Fig. 1(a), each frame included 12 key points to capture the mouse's pose and environment: 7 key points on the mouse (nose, left ear, right ear, body center, tail base, mid-tail, and tail tip) and 5 key points on the water tank (center of the platform and the four start locations: NW, N, E, and SE).

The deep convolutional neural network was trained on the DeepLabCut platform, utilizing 95 % of the data as the training set, with Resnet_50 as the backbone and applying image augmentations [15]. The cross-entropy loss values during training rapidly converged from 0.0341 to 0.0038 after 100,000 iterations and stabilized around 0.0020 after 500,000 iterations (Fig. 2(a)), indicating an effective training process. In model evaluation, the mean training error and test error were 2.37 and 2.25 pixels, respectively, with the mean test errors for all key points being less than 3 pixels (Fig. 2(b)). The likelihood distribution of key point estimations is shown in Fig. 2 (C), with only 6 out of 18,000 key points having a likelihood lower than 0.95. The mean likelihood for all key points exceeded 0.999. A visualized demo of key point estimation in our data is presented in Fig. 1(b). These results demonstrate the successful training and accurate tracking capability of MMAS, enabling its use for further analysis.

2.2. Behavior analysis

In the MMAS, automatic analysis of mouse motion was accomplished by further processing the trajectories of key points in each trial, combined with prior knowledge of the water tank. MMAS compared escape latency, cognitive score, and swimming speed across the five training days between the 5xFAD and WT mice (Fig. 3(a)–c). Escape latency, defined as the duration between the starting and stopping points, was automatically detected by the dropping and landing of the mice. The curves generated by MMAS closely matched those from the commercial video tracking software Smart 3.0 (Panlab, Harvard Apparatus, Cambridge, MA, USA) ($p = 0.4251$). Both analysis methods indicated a significant increase in escape latency in 5xFAD mice on the 2nd and 5th training days (Fig. 3(a, p) values were 0.0027 and 0.0034).

The cognitive score, reflecting an animal's 'spatial IQ', was automatically quantified by Pathfinder to determine the strategy used by mice in the MWM. Mouse path/search strategies for the platform were categorized as hippocampus-dependent or non-hippocampus-dependent. Strategies involving spatial searching, such as a 'direct path', resulted in a high cognitive score, while non-spatial strategies, such as a 'random search', resulted in a low cognitive score [6,32,33] (ranking details are described in the methods section). Compared to WT mice, 5xFAD mice showed a significant decrease in cognitive scores on the 2nd and 5th training days (Fig. 3(b, p) values were 0.0406 and 0.0117, respectively). WT mice preferred high-score search strategies, whereas AD mice scored lower. The cognitive score exhibited an inverse relationship with escape latency. These results demonstrated impaired navigation in AD mice, as they favored non-spatial search strategies and took longer to find the platform. This situation did not improve as significantly as it did in WT mice after training.

Swimming speed was calculated by dividing the cumulative distance of the body center by the escape latency. There were no

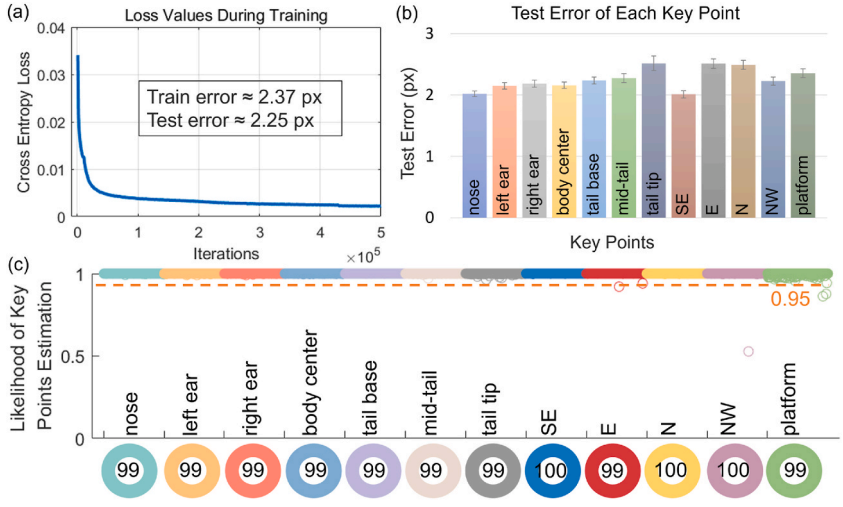

Fig. 2. Evaluation of the deep learning model. (a) Cross-entropy loss values during training, along with training and testing errors after training. (b) Test errors of each body part and environmental landmark, measured in pixels, and presented as averages with standard errors. (c) Likelihood distribution of all individual data points, represented in different colors. The dashed orange line indicates the 95 % confidence threshold for key point detection. Most points are clustered above this line. The mean values for each key point, shown at the bottom as percentages, all exceed 99.9 %.

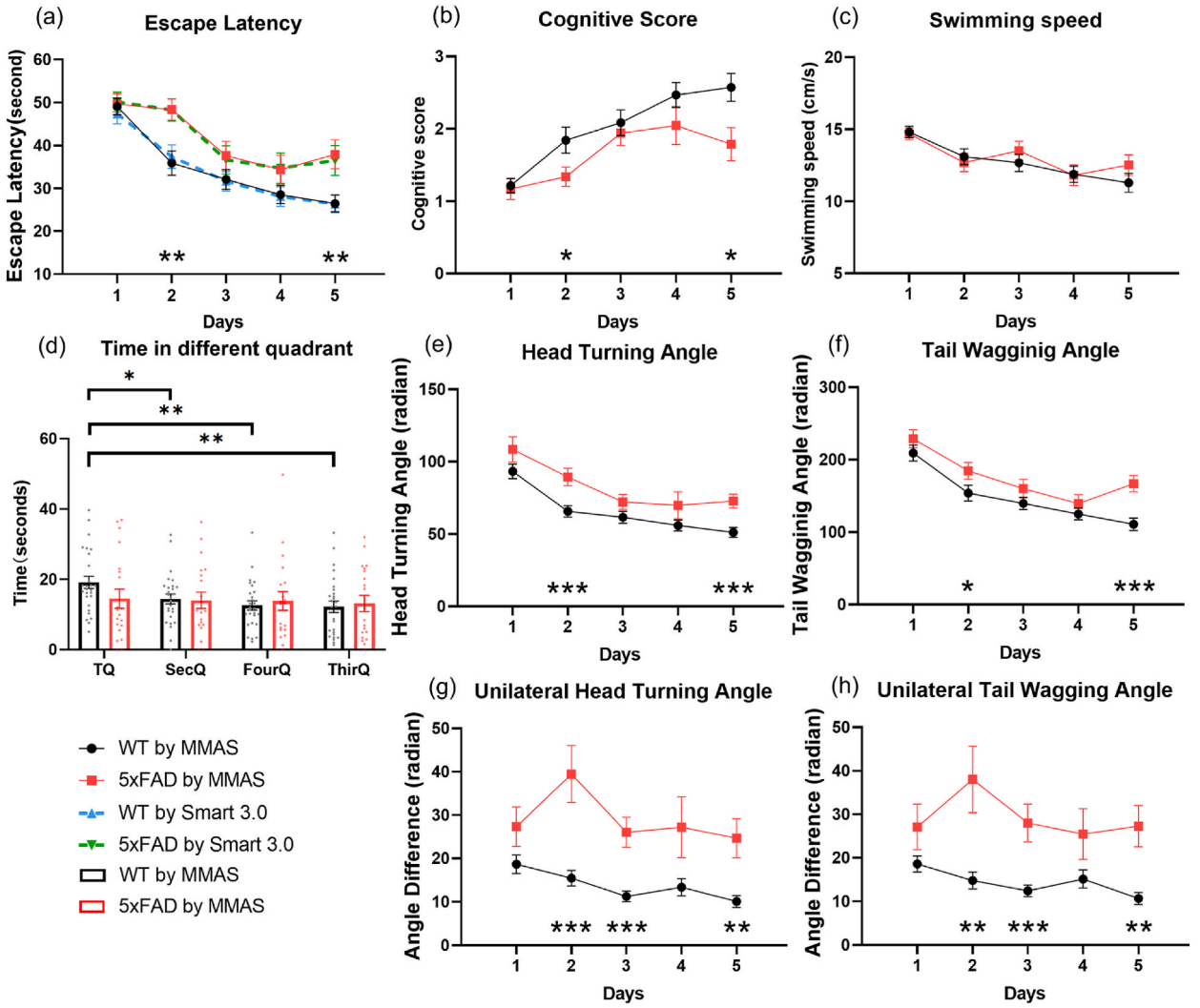

Fig. 3. Evaluation of different parameters in training and testing days. (a) Comparison of escape latency between MMAS and Smart 3.0. The solid lines denoted results from MMAS and the dashed lines represented the results from the Smart 3.0 system. A paired *t*-test suggested no significant difference. (a-c, e-h) Comparison of escape latency, cognitive score, swimming speed, HTA, TWA, UHTA and UTWA by MMAS between 5xFAD (red) and WT (black) mice across five training days. Data presented as mean ± SEM, n = 27 for WT and 20 for 5xFAD. An unpaired *t*-test was performed each day between two groups of mice. (d) Time that 5xFAD and WT mice spent respectively in four quadrants on the sixth testing day. A paired *t*-test was applied to compare the time difference that mice swam in the TQ to the other three quadrants. For all statistical analysis: *p < 0.05, **p < 0.01, ***p < 0.001. More details of individual data points can be found in Supplementray Fig. 1.

significant differences between the two groups during the training period (Fig. 3(c)), ruling out swimming ability as a factor influencing escape latency.

On the sixth testing day, the time mice spent in each quadrant was recorded. WT mice spent significantly more time in the target quadrant (TQ) than in other quadrants (p values were 0.0316, 0.0189, and 0.0043 in SecQ, FourQ, and ThirQ, respectively), indicating better memory of the platform location and training outcomes. In contrast, AD mice spent time evenly across all quadrants with no significant differences, indicating poor memory and navigation ability. These three classic parameters evaluated by MMAS robustly validate the poorer performance in spatial learning, navigation, and memory of AD mice.

2.3. Motion analysis

These behavioral parameters reflected the overall poorer performance of the AD mice in the MWM test, resulting from abnormal movements and decisions at every moment. Understanding these abnormalities—both in motion and decision-making—and their impact on behavioral disorders was crucial, as they were directly influenced by neurological impairment and could provide more sensitive indicators for AD diagnosis.

We proposed the head turning angle (HTA) and tail wagging angle (TWA) as metrics for motion analysis. These cumulative parameters indicated the extent of rotation a mouse exhibits during a trial, without considering the direction of rotation. HTA was defined as the angular movement of the nose, while TWA represented the angular movement of the tail (Fig. 1(a)). Both HTA and TWA exhibited a decreasing trend across five training days in both AD and WT mice. Significant differences were noted on the second and fifth days, correlating with escape latency and cognitive scores (HTA: $p = 0.0015$ and 0.0004; TWA: $p = 0.0652$ and 0.0002). This suggested that the abnormal angular movements contributed to the longer escape latencies and lower cognitive scores observed in AD mice.

We also introduced two additional parameters: unilateral head turning angle (UHTA) and unilateral tail wagging angle (UTWA). These parameters captured the cumulative vectors reflecting the extent of rotation in a specific direction during a trial, calculated as the absolute difference between clockwise and counterclockwise angles. Unlike the previously mentioned parameters, UHTA and UTWA (Fig. 3(g and h)) did not show a trend across the two groups, although a notable difference between the curves was observed, indicating a potential intrinsic preference for unilateral turning in AD versus WT mice. Significant differences were identified not only on the second and fifth training days but also on the third training day, with higher confidence (UHTA: $p = 0.0003$, 0.0001, and 0.0011; UTWA: $p = 0.0025$, 0.0004, and 0.0005). This suggested that these parameters were more sensitive in distinguishing between AD and WT mice across multiple experimental days.

2.4. Further evidence of abnormal motion performance

To further validate the relationship between the proposed angular parameters and classic behavioral metrics, we conducted correlation and linear regression analyses. The confusion matrix in Fig. 4 (c) revealed a strong correlation among escape latency, HTA, and TWA, all showing statistical significance. Conversely, the cognitive score demonstrated a negative correlation with these parameters. Linear regression results in Fig. 3(b–e) indicated a linear relationship between HTA and escape latency, TWA and escape latency, HTA and cognitive score, and TWA and cognitive score ($p < 0.0001$ for all). Data distribution confirmed that AD mice exhibited larger escape latencies, HTA, and TWA, along with lower cognitive scores. This strong correlation and linear regression provided compelling evidence that abnormal angular movements contribute to longer escape latencies and lower cognitive scores in AD mice. Detailed correlations for each experimental day can be found in Supplementary Fig. 2.

Changes in UHTA and UTWA during swimming were plotted in Fig. 5, including data from all trials of AD and WT mice, averages, and daily changes. Linear regression was applied to each trial, using the coefficient of determination to assess curve fluctuations. The

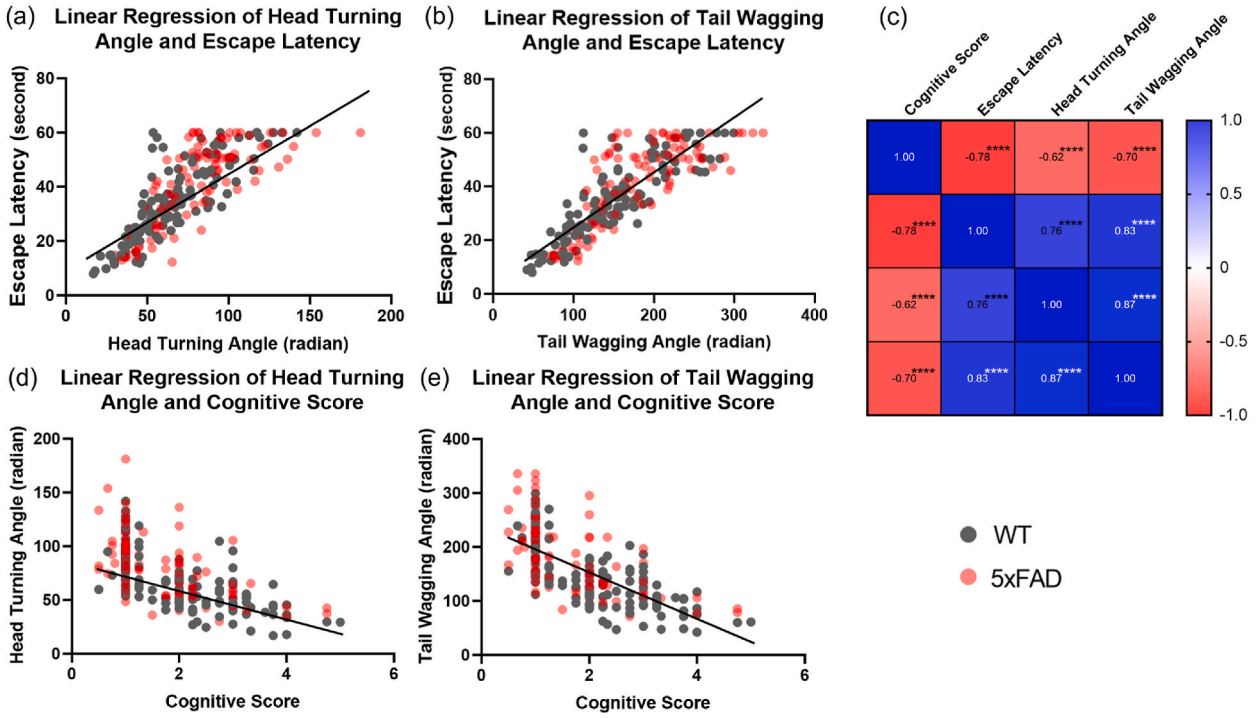

Fig. 4. Correlation and linear regression of HTA, TWA, escape latency and cognitive scores. (a-b, d-e) Linear regression results of HTA and escape latency, TWA and escape latency, HTA and cognitive score as well as TWA and cognitive score between AD (pink) and WT (grey) mice. Each dot denoted individual data point. The line of regression was plotted too. (c) Confusion matrix among cognitive score, escape latency, HTA and TWA. Different colors and numbers in the cells denoted the positive/negative correlation and coefficients of two parameters. For all statistical results: ****$p < 0.0001$.

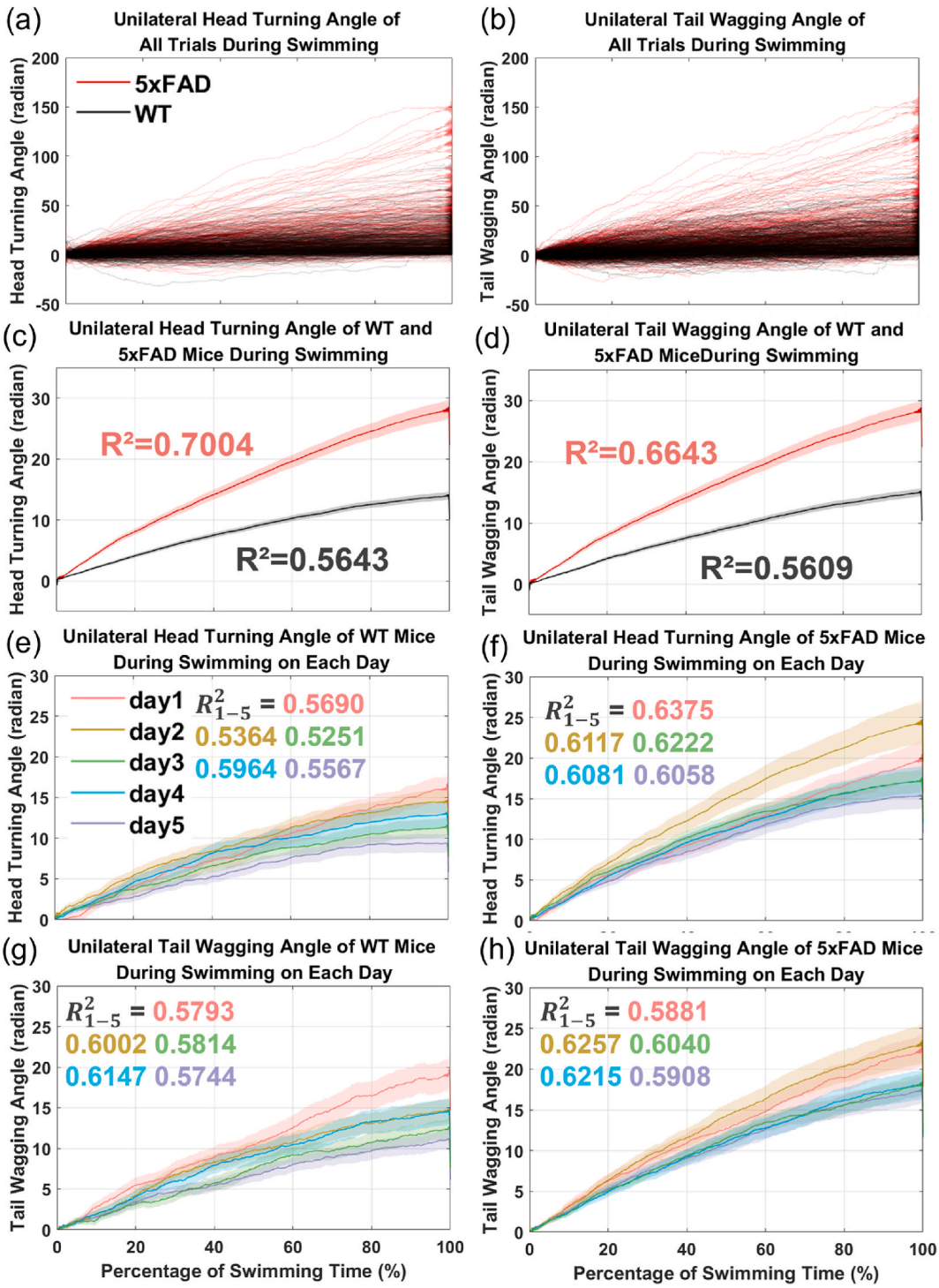

Fig. 5. UHTA and UTWA changes of AD or WT mice during swimming. The horizontal axis was percentage of swimming time, which were normalized from putting the mice into the water tank to finding the platform or the time was up. The curves were taken negative values when the last value was negative to make sure the final unilateral angles were positive. (a, b) Angular changes in all trials. Each red line denoted one AD mouse. And black lines were for WT mice. (c, d) The average (solid line) and standard error (area). Red and black denoted AD and WT mice respectively. The mean R^2 from linear regression of all the trials were noted in the corresponding color next to the AD or WT curves. (e–h) Angular changes in five training days. Solid lines denoted the average and areas in the same color denoted the corresponding standard error. Mean R^2 and curves on each day were presented in five colors as shown in the legend.

distribution of UHTA and UTWA in Fig. 5(a, b) indicated that AD mice had steeper slopes, while WT mice displayed smaller fluctuations. Average values in Fig. 5(c, d) further supported this finding, with AD mice showing a higher mean R^2 than WT mice, suggesting better linear fitting and less deviation. In essence, AD mice exhibited a preference for continuous unilateral turning and wagging. Consistent results were observed across daily performances, as shown in Fig. 5(e–h), where both UHTA and UTWA revealed higher slopes and greater mean R^2 for AD mice, highlighting a prevalent unilateral movement preference as a significant distinction in AD mice.

3. Discussions

Spatial disorientation and navigation impairments are among the earliest indicators leading to an Alzheimer's disease (AD) diagnosis, supported by substantial evidence [4,32]. Classic behavioral parameters—such as escape latency, search strategies, and cognitive scores—have been extensively utilized in Morris Water Maze (MWM) tests to identify these deficits [25,33]. With advancements in deep learning, automatic pose estimation and motion analysis for swimming mice can be realized, enabling a deeper understanding of how AD impacts motion and subsequently leads to behavioral changes.

The rapid convergence of training loss indicates that our model effectively captures patterns and reduces errors between predicted and actual values, demonstrating the appropriateness of key point selection. In both the training and testing sets, evaluation errors were only 0.30 % and 0.48 % of the image resolution, respectively. And the test errors are evenly distributed on each key point with a very high likelihood, suggesting that the model is not overfitted and possesses strong tracking capabilities for multiple body parts. This accuracy enables the implementation of our automated system for further analysis. Notably, when compared to the commercial Smart 3.0 system in terms of escape latency, no significant differences were found, underscoring the precision and reliability of our automated approach.

Importantly, we observed no significant difference in swimming speed between the two groups, ruling out swimming ability as a factor influencing escape latency. The reduction in time taken to locate the platform over successive training days indicates that both groups were learning to escape. However, the AD group exhibited a slower rate of improvement compared to the WT group, suggesting deficits in spatial learning ability. Furthermore, cognitive scores revealed that WT mice employed high-scoring search strategies, predominantly spatial strategies that rely on hippocampal function, while AD mice demonstrated lower scores. These findings highlight the navigation impairments in AD mice, who tended to favor non-spatial and non-hippocampal-dependent strategies, with little improvement observed after training. On the sixth testing day, results further confirmed memory impairments in AD mice. WT mice spent significantly more time in the target quadrant (TQ) compared to other quadrants, indicating superior recall of the platform's location and training outcomes. In contrast, AD mice exhibited an even distribution of time spent across all quadrants, reflecting poor memory and navigation abilities. Collectively, these three classic parameters robustly validate the spatial learning, navigation, and memory impairments observed in the AD group.

These behavioral parameters reflect the overall poorer performance of AD mice in the Morris Water Maze (MWM) test, resulting from abnormal movements and decision-making at every moment. Understanding these abnormal motions and decisions is crucial, as they are directly influenced by neurological impairment and could serve as sensitive indicators for AD diagnosis. The results for head turning angle (HTA) and tail wagging angle (TWA) indicate that AD mice exhibited larger angular movements and a slower decrease in both metrics over five training days. Notably, significant differences in the WT group were observed on the second and third days, correlating with escape latency and cognitive scores. This suggests that abnormal angular movements may contribute to the longer escape latencies and lower cognitive scores observed in AD mice, as well-targeted mice navigate more directly to their goals with minimal turns, requiring good spatial memory and path-planning capabilities.

Further analysis of unilateral head turning angle (UHTA) and unilateral tail wagging angle (UTWA) reveals that AD mice are more prone to unilateral rotations, suggesting a tendency to spin aimlessly in small circles, indicative of spatial disorientation. This inefficient strategy reflects reduced exploration and searching capabilities. In contrast, bilateral turning and larger radius turns can cover more area, facilitating platform discovery. While the differences between UHTA and UTWA curves are clear, they do not show a consistent upward or downward trend after training, suggesting these metrics might represent intrinsic differences between AD and WT mice. The consistent preference for unilateral turning among AD mice, evidenced by less fluctuation in their curves, highlights a behavioral pattern potentially linked to neurological impairments. This aimless swimming could result from an inability to effectively organize search routes. An alternative interpretation could involve a left-right imbalance in AD mice, supported by reports of balance dysfunction in AD models, as indicated by their poorer performance in balance tasks [29,30,34,35]. While our 6-month-old AD mice may not show significant deficits in swimming speed, balance impairments could lead to altered swimming trajectories and UHTA/UTWA values, causing a tendency to swim toward the imbalanced side. Both interpretations converge on the conclusion that the increased UHTA and UTWA in AD mice are consistent with neurological impairments linked to behavioral disorders. Importantly, these parameters demonstrated greater sensitivity in distinguishing AD from WT mice, with significant differences noted not only on the second and fifth training days but also on the third day with high confidence. The lack of clear trends across days suggests that these metrics can effectively differentiate between the two groups with fewer experimental trials. The potential of these parameters as indicators for drug testing and early AD diagnosis is substantial.

In summary, we developed a modular motion analysis system for detecting spatial disorientation in the MWM test using deep learning, achieving comparable accuracy to commercial software while excelling in multi-body part analysis. This system revealed that the spatial searching impairment in AD mice led to aimless turning decisions, resulting in increased steering and unilateral turning angles, ultimately worsening behavioral performance. The motion curves further illustrated that these deficits consistently affected turning movements and decision-making during swimming. Moreover, the sensitivity of these angular parameters in detecting

differences without requiring extended MWM testing holds promise for efficient evaluation of preclinical drug effects in Alzheimer's and other neurological disorders.

4. Limitations of the study

Several limitations should be addressed in future research. First, increasing the sample size could yield more robust insights into cognitive domains related to identification. Second, enhancing the diversity of the dataset is essential; this could involve including AD mice from various strains, ages, genetic mutations, and medical interventions, which would broaden the generalizability of our findings. Third, incorporating biological tests alongside motion analysis could enhance the completeness and interpretability of the evidence. Finally, utilizing close-up and lateral camera recordings to track and analyze the movement of the mice's paws during swimming could provide additional evidence and insights into the observed unidirectional rotation preference.

5. Method details

5.1. AD mice

In this study, we used transgenic 5xFAD mice models, obtained from Jackson Laboratory (stock no: 34848), which do not carry the retina degeneration allele Pde6brd1. These 5xFAD transgenic mice overexpress familial Alzheimer's disease mutations of human APP (695) with the Swedish (K670N/M671L), Florida (I716V), and London (V717I) mutations, as well as human PS1 with two FAD mutations, M146L and L286V. To maintain the colony, C57BL/6J mice were purchased from the Laboratory Animal Unit (LAU) of the University of Hong Kong and bred with 5xFAD mice. Both hemizygous 5xFAD mice and non-transgenic wild-type littermates were used. The mice were housed in groups of no more than four per cage and kept on a 12-h light/12-h dark cycle, with all experiments conducted during the light phase. All procedures, including handling, were performed in accordance with the National Institutes of Health guide for the care and use of laboratory animals and the Animals (Control of Experiments) Ordinance, Hong Kong, China. The Committee on the Use of Live Animals in Teaching and Research of the University of Hong Kong (CULATR, no: 5724-21) approved all animal work. Efforts were made to minimize the number of animals used and their suffering. This study included a total of 27 wild-type (WT) mice and 20 5xFAD mice, all aged 6 months.

5.2. Morris water maze

Spatial learning and memory were evaluated using the MWM following the established protocol [8]. The MWM was conducted in a circular pool with a diameter of 90 cm and a height of 60 cm, filled with white opaque water maintained at approximately 22 °C. Reference cues of various colors and shapes were placed along the walls surrounding the pool. During the initial training phase, a platform (10 cm in diameter) was positioned in a target quadrant, submerged 1 cm below the water surface. Two days prior to the commencement of behavioral studies, the mice were acclimated to the environment and handling procedures. Mice were removed from the cage rack, placed on the lab bench, and handled by grasping the tail for no more than 5 s each time, allowing them to acclimate over two consecutive days.

During the trials, mice were placed into the tank facing the side wall and near the edge at one of four randomly chosen points. They were given 60 s to locate the platform, and if unsuccessful, were gently guided to it. Mice were allowed to remain on the platform for 15 s for training purposes. Four trials were conducted daily with a 1-h intertrial interval. Between trials, mice were gently dried and warmed on a heating pad. The training phase lasted for 5 days, with videos recorded for subsequent analysis. The escape latency for mice that failed to find the platform was recorded as 60 s. On the sixth day, the platform was removed, and the mice were placed in the pool from the opposite side of the previous platform location. The number of crossings over the former platform area was recorded. On average, around 20 min of video footage was recorded for each mouse.

5.3. Pose estimation and environment detection

Pose estimation and environment detection in MMAS were achieved simultaneously by training a deep neural network using DeepLabCut [15]. An experienced researcher manually labeled 1500 images of swimming mice, with 95 % of the dataset used for training and the remaining 5 % for testing. These images were keyframes automatically extracted from experimental videos using the k-means algorithm. In each frame, seven key points were labeled on the mouse: the nose, left ear, right ear, body center, tail base, mid-tail, and tail tip. Additionally, five markers were labeled on the water tank, including the center of the platform and four start locations (NW, N, E, and SE) (Fig. 1). We utilized Resnet_50 as the network backbone and trained the model over 500,000 iterations with image augmentation. Post-training, the model was evaluated and selected based on minimum pixel errors in both the training and testing sets. This model was then used to analyze each experimental video to identify key points in every frame. The test error for each key point and the likelihood of key point estimation were also taken into account.

To validate MMAS, the experimental videos were also processed using the commercial video tracking software Smart v3.0 (Panlab, Harvard Apparatus, Cambridge, MA, USA) according to the manual's instructions. For each video, the size and location of the water tank and platform, as well as the start and end times, were manually labeled based on the setup for each trial. Additionally, the body center of each mouse was manually labeled in the videos.

5.4. Behavior and motion analysis

In MMAS, automatic mouse motion analysis was achieved by further processing the trajectories of key points in each trial, utilizing prior knowledge of the water tank. The coordinates of key points on the water tank were finalized using median values. The diameter of the water tank, measured as the distance between SE and NW, was 90 cm, allowing all measurements to be analyzed on a physical scale.

To calculate escape latency in MMAS, the starting and ending points of the swimming were first manually set in Smart 3.0. The footage of placing the mice in the water tank was often recorded, but hand occlusion frequently caused incorrect detection and significant errors. To automate this process, we filtered the starting frames where the body center's speed exceeded 30 cm/s, determining the starting moment based on statistical calculations of our mice's swimming speed and relevant reports. The ending moment was identified when the body center entered the platform area with a diameter of 10 cm, and escape latency was defined as the duration between these two time points. This classic parameter was also compared with results from Smart 3.0 for validation. Swimming speed was then calculated by dividing the cumulative distance traveled by the body center by the escape latency. On the sixth testing day, the water tank was divided into four quadrants: the target quadrant (TQ) with the platform at its center, the second and third quadrants (SecQ and ThirQ) adjacent to TQ, and the fourth quadrant (FourQ) opposite TQ (Fig. 1(a)). The cumulative time each mouse spent in each quadrant was also calculated.

Spatial navigation search strategies were estimated using the open-source software Pathfinder [32]. The spatial parameters were adjusted according to our experimental setup: goal position [x/y] based on the coordinates of the platform center in each trial; goal diameter: 10 cm; maze diameter: 90 cm; maze center [x/y] based on the coordinates of the midpoints of SE and NW in each trial; angular corridor width: 40°; chaining annulus width: 15 cm; and thigmotaxis zone size: 10 cm. The output included eight different search strategies, each corresponding to different cognitive scores: direct path = 6; directed search = 5; focal search = 4; indirect search = 4; chaining = 3; scanning = 2; random search = 1; and thigmotaxis = 0 [6,33]. The daily cognitive scores for each mouse were calculated as the average of multiple experiments per day. The final cognitive score for each day was averaged across all the mice.

HTA and TWA were cumulative metrics that measured the extent of rotation in a single trial, without considering the rotation direction. As shown in Fig. 1(a), HTA was defined as the angle formed by the nose before and after movement, relative to the butt. Similarly, TWA was defined by the angles at the butt and tail tip before and after movement. UHTA and UTWA were cumulative vectors indicating the extent of rotation in a specific direction during a trial. These were calculated as the absolute difference between clockwise and counterclockwise rotation angles. Changes in UHTA and UTWA during swimming were plotted, including all trials for both AD and WT mice, as well as daily averages and changes in Fig. 3. The horizontal axis represented the percentage of swimming time, normalized from the moment the mice were placed in the water tank until they found the platform or the time expired in Fig. 4. The curves were adjusted to ensure the final unilateral angles were positive, with negative values taken when the last value was negative as shown in Fig. 5.

5.5. Statistical analysis

Statistical analyses and plotting were conducted using GraphPad Prism 9.00 and MATLAB R2018a. A paired *t*-test was used to analyze the escape latency results from MMAS and Smart 3.0. During the first five training days, an unpaired *t*-test compared the differences between WT and AD mice each day. On the sixth testing day, a paired *t*-test compared the time mice spent swimming in the target quadrant (TQ) versus the other three quadrants. For escape latency, cognitive score, HTA, and TWA, Pearson correlation was initially applied, followed by linear regression on HTA and TWA-related parameters. Significance levels were defined as follows: ****$p < 0.0001$, ***$p < 0.001$, **$p < 0.01$, and * $p < 0.05$. Linear regression was also applied to each trial of UHTA or UTWA changes during swimming, with the coefficient of determination used to estimate the fluctuation of each curve.

CRediT authorship contribution statement

Yuanhao Liang: Writing – original draft, Visualization, Validation, Software, Methodology, Investigation, Conceptualization. **Zhongqing Sun:** Writing – original draft, Validation, Methodology, Investigation, Formal analysis, Data curation, Conceptualization. **Kin Chiu:** Writing – review & editing, Supervision, Resources, Project administration, Investigation, Funding acquisition, Data curation, Conceptualization. **Yong Hu:** Writing – review & editing, Supervision, Resources, Project administration, Methodology, Investigation, Funding acquisition, Conceptualization.

Ethics approval and consent to participate

All animal work was approved by the Committee on the Use of Live Animals in Teaching and Research of the University of Hong Kong (CULATR, no: 5724-21).

Data and code availability

The data collected and analyzed in the present study are publicly available:
The codes are available to the public on GitHub: https://github.com/yhliang98/MMAS.

Funding

This work was supported by Shenzhen science and technology program (GJHZ20220913143408015), Sanming Project of Medicine in Shenzhen, China (No. SZSM202211004), and Shenzhen Key Medical Discipline Construction Fund (No. SZXK2020084). The funding sources had no role in study conception and design, data analysis or interpretation, paper writing or deciding to submit this paper for publication.

Declaration of competing interest

The authors declare the following financial interests/personal relationships which may be considered as potential competing interests:Yong Hu reports financial support, administrative support, article publishing charges, equipment, drugs, or supplies, and travel were provided by Shenzhen science and technology program. Yong Hu reports financial support, administrative support, article publishing charges, equipment, drugs, or supplies, and travel were provided by Sanming Project of Medicine in Shenzhen, China. Yong Hu reports financial support, administrative support, article publishing charges, equipment, drugs, or supplies, and travel were provided by Shenzhen Key Medical Discipline Construction Fund. If there are other authors, they declare that they have no known competing financial interests or personal relationships that could have appeared to influence the work reported in this paper.

Acknowledgments

The authors acknowledge the great support of funding, facilities, and helpful comments from the Midstream Research Program for Universities, Hong Kong, China, No. MRP-092-17X, the Sanming Project of Medicine in Shenzhen, China (No. SZSM202211004), and Li Kai Shing Faculty of Medicine, The University of Hong Kong, Hong Kong, China. Thank for the technique support by AI and Big Data Lab, The University of Hong Kong-Shenzhen Hospital.

Appendix A. Supplementary data

Supplementary data to this article can be found online at https://doi.org/10.1016/j.heliyon.2024.e39353.

References

[1] C. Lynch, World Alzheimer Report 2019: attitudes to dementia, a global survey: public health: engaging people in ADRD research, Alzheimer's Dementia 16 (2020) e038255.
[2] S. Sutoko, A. Masuda, A. Kandori, H. Sasaguri, T. Saito, T.C. Saido, T. Funane, Early identification of Alzheimer's disease in mouse models: application of deep neural network algorithm to cognitive behavioral parameters, iScience 24 (3) (2021).
[3] J. Cummings, Y. Zhou, G. Lee, K. Zhong, J. Fonseca, F. Cheng, Alzheimer's disease drug development pipeline: 2023, Alzheimer's Dementia: Translational Research & Clinical Interventions 9 (2) (2023) e12385.
[4] V.W. Henderson, W. Mack, B.W. Williams, Spatial disorientation in Alzheimer's disease, Arch. Neurol. 46 (4) (1989) 391–394.
[5] V. Puthusseryppady, S. Morrissey, H. Spiers, M. Patel, M. Hornberger, Predicting real world spatial disorientation in Alzheimer's disease patients using virtual reality navigation tests, Sci. Rep. 12 (1) (2022) 13397.
[6] N. Curdt, F.W. Schmitt, C. Bouter, T. Iseni, H.C. Weile, B. Altunok, N. Beindorff, T.A. Bayer, M.B. Cooke, Y. Bouter, Search strategy analysis of Tg4-42 Alzheimer Mice in the Morris Water Maze reveals early spatial navigation deficits, Sci. Rep. 12 (1) (2022) 5451.
[7] R. D'Hooge, P.P. De Deyn, Applications of the Morris water maze in the study of learning and memory, Brain Res. Rev. 36 (1) (2001) 60–90.
[8] C.V. Vorhees, M.T. Williams, Morris water maze: procedures for assessing spatial and related forms of learning and memory, Nat. Protoc. 1 (2) (2006) 848–858.
[9] S.J. Webster, A.D. Bachstetter, P.T. Nelson, F.A. Schmitt, L.J. Van Eldik, Using mice to model Alzheimer's dementia: an overview of the clinical disease and the preclinical behavioral changes in 10 mouse models, Front. Genet. 5 (2014) 88.
[10] K. Bromley-Brits, Y. Deng, W. Song, Morris water maze test for learning and memory deficits in Alzheimer's disease model mice, JoVE (53) (2011) e2920.
[11] A. Rodríguez, A. Ortega-Álvaro, A. Sola, J. A. Micó, and O. Trelles, "Automatic Tracking Analysis in Morris Water Maze Biomedical Videos." pp. 647-652.
[12] T. Connie, T.B. Aderinola, T.S. Ong, M.K.O. Goh, B. Erfianto, B. Purnama, Pose-based gait analysis for diagnosis of Parkinson's disease, Algorithms 15 (12) (2022) 474.
[13] G. T. Acevedo Trebbau, A. Bandini, and D. L. Guarin, "Video-Based Hand Pose Estimation for Remote Assessment of Bradykinesia in Parkinson's Disease." pp. 241-252.
[14] D. Wang, C. Zouaoui, J. Jang, H. Drira, and H. Seo, "Video-based Gait Analysis for Assessing Alzheimer's Disease and Dementia with Lewy Bodies." pp. 72-82.
[15] A. Mathis, P. Mamidanna, K.M. Cury, T. Abe, V.N. Murthy, M.W. Mathis, M. Bethge, DeepLabCut: markerless pose estimation of user-defined body parts with deep learning, Nat. Neurosci. 21 (9) (2018) 1281–1289.
[16] T.D. Pereira, D.E. Aldarondo, L. Willmore, M. Kislin, S.S.-H. Wang, M. Murthy, J.W. Shaevitz, Fast animal pose estimation using deep neural networks, Nat. Methods 16 (1) (2019) 117–125.
[17] G. Salem, J. Krynitsky, M. Hayes, T. Pohida, X. Burgos-Artizzu, Three-dimensional pose estimation for laboratory mouse from monocular images, IEEE Trans. Image Process. 28 (9) (2019) 4273–4287.
[18] K. Sheppard, J. Gardin, G.S. Sabnis, A. Peer, M. Darrell, S. Deats, B. Geuther, C.M. Lutz, V. Kumar, Stride-level analysis of mouse open field behavior using deep-learning-based pose estimation, Cell Rep. 38 (2) (2022).
[19] R.Z. Weber, G. Mulders, J. Kaiser, C. Tackenberg, R. Rust, Deep learning-based behavioral profiling of rodent stroke recovery, BMC Biol. 20 (1) (2022) 1–19.
[20] T. Leroy, M. Silva, R. D'Hooge, J.-M. Aerts, D. Berckmans, Automated gait analysis in the open-field test for laboratory mice, Behav. Res. Methods 41 (2009) 148–153.
[21] M.T. Koh, R.P. Haberman, S. Foti, T.J. McCown, M. Gallagher, Treatment strategies targeting excess hippocampal activity benefit aged rats with cognitive impairment, Neuropsychopharmacology 35 (4) (2010) 1016–1025.
[22] H. Tian, N. Ding, M. Guo, S. Wang, Z. Wang, H. Liu, J. Yang, Y. Li, J. Ren, J. Jiang, Analysis of learning and memory ability in an Alzheimer's disease mouse model using the Morris water maze, JoVE (152) (2019) e60055.

[23] M.G. Forero, N.C. Hernández, C.M. Morera, L.A. Aguilar, R. Aquino, L.E. Baquedano, A new automatic method for tracking rats in the Morris water maze, Heliyon 9 (7) (2023) e18367.
[24] L.E. Berkowitz, R.E. Harvey, E. Drake, S.M. Thompson, B.J. Clark, Progressive impairment of directional and spatially precise trajectories by TgF344-Alzheimer's disease rats in the Morris Water Task, Sci. Rep. 8 (1) (2018) 16153.
[25] T. Illouz, R. Madar, Y. Louzon, K.J. Griffioen, E. Okun, Unraveling cognitive traits using the Morris water maze unbiased strategy classification (MUST-C) algorithm, Brain Behav. Immun. 52 (2016) 132–144.
[26] O. Wirths, T.A. Bayer, Motor impairment in Alzheimer's disease and transgenic Alzheimer's disease mouse models, Genes Brain Behav 7 (Suppl 1) (2008) 1, 5, Feb.
[27] L.Z. Gras, S.F. Kanaan, J.M. McDowd, Y.M. Colgrove, J. Burns, P.S. Pohl, Balance and gait of adults with very mild Alzheimer's disease, J. Geriatr. Phys. Ther. 38 (1) (2001) 1, 2015.
[28] S. O'keeffe, H. Kazeem, R. Philpott, J. Playfer, M. Gosney, M. Lye, Gait disturbance in Alzheimer's disease: a clinical study, Age Ageing 25 (4) (1996) 313–316.
[29] T.P. O'Leary, A. Robertson, P.H. Chipman, V.F. Rafuse, R.E. Brown, Motor function deficits in the 12 month-old female 5xFAD mouse model of Alzheimer's disease, Behav. Brain Res. 337 (2018) 256–263.
[30] S. Jawhar, A. Trawicka, C. Jenneckens, T.A. Bayer, O. Wirths, Motor deficits, neuron loss, and reduced anxiety coinciding with axonal degeneration and intraneuronal Abeta aggregation in the 5XFAD mouse model of Alzheimer's disease, Neurobiol. Aging 33 (1) (2012), 196 e29-40, Jan.
[31] T.H. Chu, K. Cummins, J.S. Sparling, S. Tsutsui, C. Brideau, K.P.R. Nilsson, J.T. Joseph, P.K. Stys, Axonal and myelinic pathology in 5xFAD Alzheimer's mouse spinal cord, PLoS One 12 (11) (2017) e0188218.
[32] J.M. Long, D.M. Holtzman, Alzheimer disease: an update on pathobiology and treatment strategies, Cell 179 (2) (Oct 3, 2019) 312–339.
[33] C.Q. Sánchez, F.W. Schmitt, N. Curdt, A.C. Westhoff, I.W.H. Bänfer, T.A. Bayer, Y. Bouter, Search strategy analysis of 5xFAD alzheimer mice in the Morris water maze reveals sex-and age-specific spatial navigation deficits, Biomedicines 11 (2) (2023) 599.
[34] O. Wirths, H. Breyhan, S. Schäfer, C. Roth, T.A. Bayer, Deficits in working memory and motor performance in the APP/PS1ki mouse model for Alzheimer's disease, Neurobiol. Aging 29 (6) (2008) 891–901. Jun.
[35] T. O'Leary, A. Robertson, P. Chipman, V. Rafuse, R. Brown, Motor function deficits in the 12 month-old female 5xFAD mouse model of Alzheimer's disease, Behav. Brain Res. 337 (2018) 256–263.